Mechanism of Water Oxidation Catalyzed by the μ-Oxo Dimer $[(bpy)_2(OH_2)Ru^{III}ORu^{III}(OH_2)(bpy)_2]^{4+}$

Chris W. Chronister, Robert A. Binstead, Jinfeng Ni, and Thomas J. Meyer*

Department of Chemistry, University of North Carolina at Chapel Hill, Chapel Hill, North Carolina 27599-3290

Received April 3, 1997

Well-defined catalysts for water oxidation are rare. This is not surprising given the thermodynamic and mechanistic requirements of the reaction, eq 1. The reported catalysts include

$$O_2 + 4H^+ + 4e^- \rightarrow 2H_2O \qquad E^\circ = +1.23 \text{ V vs NHE} \quad (1)$$

an *o*-phenylene-bridged porphyrin manganese dimer and the blue ruthenium dimer ($[(bpy)_2(H_2O)Ru^{III}ORu^{III}(H_2O)(bpy)_2](ClO_4)_4$; bpy is 2,2′-bipyridine) and its derivatives.[1−3] ***Warning:*** *Perchlorate salts are hazardous because of the possibility of explosion!* Understanding the mechanism or mechanisms of these reactions may be of relevance to oxygen evolution at the oxygen-evolving complex (OEC) of photosystem II.[4] We report here that water oxidation by the blue dimer is a complex process featuring stepwise redox cycling among five different oxidation states of the catalyst and an oxygen-evolving step that is not rate determining.

The $Ru^{III}ORu^{III}$ and $Ru^{III}ORu^{IV}$ forms of the blue dimer have been characterized structurally.[2b,5,6] The higher oxidation state, $Ru^{IV}ORu^{V}$, can be generated by chemical or electrochemical oxidation of $Ru^{III}ORu^{IV}$, for which electrolysis at 1.0 V vs SSCE at pH 6 was reported to occur with $n = 2$ and loss of three protons ($\lambda_{max} = 490$ nm, $\epsilon = 9.7 \times 10^3$ M^{-1} cm^{-1}).[2c] We have since found that those conditions produce incomplete oxidation. Electrolysis of $Ru^{III}ORu^{IV}$ (8×10^{-4} M, 0.1 M $NaCF_3SO_3$, pH 5.9) at 0.7 V vs $Hg/HgSO_4$ (∼1.1 V vs SSCE) gave a final spectrum with $\lambda_{max} = 500$ nm ($\epsilon \sim 7 \times 10^3$ M^{-1} cm^{-1}). Protonation of $Ru^{IV}ORu^{V}$ occurred instantaneously upon 1:1 mixing with 2 M HCF_3SO_3 ($\lambda_{max} = 482$ nm, $\epsilon \sim 1.6 \times 10^4$ M^{-1} cm^{-1}).[7] The same result was obtained by stoichiometric oxidation with Ce^{IV} at pH 0 (5−25 °C).

In Figure 1a is shown the absorbance−time trace that occurs following addition of 2 equiv of Ce^{IV} to 3.5×10^{-5} M $Ru^{III}ORu^{IV}$ ($\lambda_{max} = 444$ nm) in 1 M $HClO_4$. In Figure 1b,c are shown the results of the application of global kinetic analysis

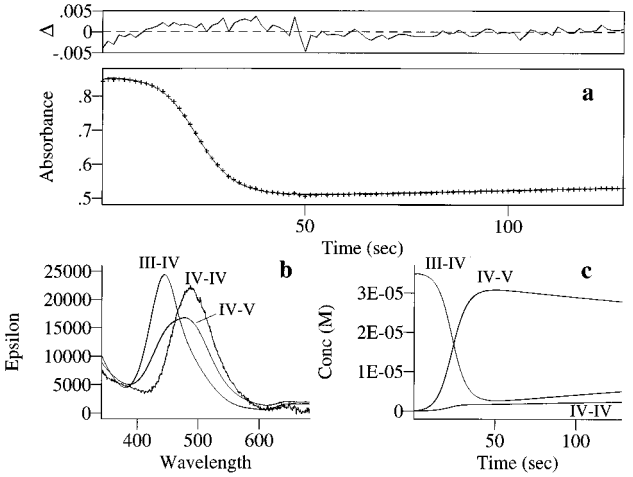

Figure 1. Kinetic behavior observed for addition of 2 equiv of Ce^{IV} to a solution 3.5×10^{-5} M in $Ru^{III}ORu^{IV}$ (1 M $HClO_4$, 25 °C, $l = 1$ cm): (a) absorbance vs time trace at 444 nm (+++), fitted curve (−), and residuals (Δ); (b) predicted spectra from the global fit; (c) predicted concentration profiles from the global fit.

to the spectral changes according to Scheme 1, producing the predicted spectra and distribution of the dominant oxidation states during the course of the reaction.[8] The species designated as $Ru^{IV}ORu^{IV}$ never builds up appreciably, and its derived spectrum is subject to considerable uncertainty.[9]

At 5 °C in 1 M $HClO_4$, addition of 3 equiv of Ce^{IV} to a 0.5 mM solution of $Ru^{III}ORu^{IV}$ results in the appearance of a black microparticulate suspension having λ_{max} values near 400 and 600 nm. In the resonance Raman spectrum at 77 K (50 mW excitation at 488 nm) significant resonance enhancements were observed for ν_{sym} at 353 cm^{-1} and a band at 816 cm^{-1} that was assigned by Hurst *et al.* as a terminal $\nu_{Ru=O}$ stretch.[2e] The black

(1) (a) Naruta, Y.; Masa-aki, S.; Sasaki, T. *Angew. Chem., Int. Ed. Engl.* **1994**, *33*, 1839.
(2) (a) Gersten, S. W.; Samuels, G. J.; Meyer, T. J. *J. Am. Chem. Soc.* **1982**, *104*, 4029. (b) Gilbert, J. A.; Eggleston, D. S.; Murphy, W. R., Jr.; Geselowitz, D. A.; Gersten, S. W.; Hodgson, D. J.; Meyer, T. J. *J. Am. Chem. Soc.* **1985**, *107*, 3855. (c) Raven, S. J.; Meyer, T. J. *Inorg. Chem.* **1988**, *27*, 4478. (d) Geselowitz, D.; Meyer, T. J. *Inorg. Chem.* **1990**, *29*, 3894. (e) Hurst, J. K.; Zhou, J; Lei, Y. *Inorg. Chem.* **1992**, *31*, 1010. (f) Lei, Y.; Hurst, J. K. *Inorg. Chem.* **1994**, *33*, 4460. (g) Lei, Y.; Hurst, J. K. *Inorg. Chim. Acta* **1994**, *226*, 179.
(3) (a) Rotzinger, F. P.; Munavalli, S.; Comte, P.; Hurst, J. K.; Gratzel, M.; Pern, F. J.; Frank, A. J. *J. Am. Chem. Soc.* **1987**, *109*, 6619. (b) Nazeeruddin, M. K.; Rotzinger, F. P.; Comte, P.; Gratzel, M. *J. Chem. Soc., Chem. Commun.* **1988**, 872. (c) Comte, P.; Nazeeruddin, M. K.; Rotzinger, F. P.; Frank, A. J.; Gratzel, M. *J. Mol. Catal.* **1989**, *52*, 63. (d) Petach, H. H.; Elliott, C. M. *J. Electrochem. Soc.* **1992**, *139*, 2217. (e) Lai, Y.-K.; Wong, K.-Y. *J. Electrochem. Soc.* **1995**, *380*, 193.
(4) (a) Brudvig, G. W.; Crabtree, R. H. *Proc. Natl. Acad. Sci. U.S.A.* **1986**, *83*, 4586. (b) Brudvig, G. W.; Crabtree, R. H. *Prog. Inorg. Chem.* **1989**, *37*, 99. (c) Christou, G. *Acc. Chem. Res.* **1989**, *22*, 328. (d) Pecoraro, V. L. *Photochem. Photobiol.* **1988**, *48*, 249. (e) Wieghardt, K. *Angew. Chem., Int. Ed. Engl.* **1989**, *28*, 1153. (f) DeRose, V. J.; Mukerji, I.; Latimer, M. J.; Yachandra, V. K.; Sauer, K.; Klein, M. P. *J. Am. Chem. Soc.* **1994**, *116*, 5239.
(5) Schoonover, J. R.; Ni, J.; Roecker, L.; White, P. S.; Meyer, T. J. *Inorg. Chem.* **1996**, *35*, 5885.
(6) The oxidation state designations, $Ru^{III}ORu^{IV}$, *etc.*, are only intended to convey electron content. There is strong electronic coupling through the μ-oxo bridge, and the assignment of oxidation states is equivocal.
(7) Rapid-scanning, stopped-flow kinetics experiments showed no risetime for the initial spectral change that occurs upon mixing $Ru^{IV}ORu^{V}$ (pH 6) with acid. This was misinterpreted in ref 2c as very rapid disproportionation of $Ru^{IV}ORu^{V}$. While the electrochemical results in ref 2b indicate that $Ru^{IV}ORu^{V}$ is thermodynamically unstable at pH 0, the kinetics for disproportionation are quite slow, requiring several hours for complete recovery of $Ru^{III}ORu^{IV}$ via the sequence of reactions shown in Scheme 1.
(8) Spectral-kinetic data were obtained with a Hi-Tech SF-61MX stopped-flow/diode array spectrophotometer and processed by use of the program SPECFIT (Spectrum Software Associates, Chapel Hill, NC). For details of the method, see: Stultz, L. K.; Binstead, R. A.; Reynolds, M. S.; Meyer, T. J. *J. Am. Chem. Soc.* **1995**, *117*, 2520 and references therein.
(9) (a) For $Ru^{IV}ORuO^{IV}$ the oxidation state description could equally well be $Ru^{III}ORu^{V}$ (see ref 2c). (b) Singular value decomposition analysis of the spectral-kinetic data revealed the presence of three colorimetric components, though the third was quite small. The inclusion of $Ru^{IV}ORu^{IV}$ as a third colored species in the global kinetic analysis improved the fit, but its spectrum should not be considered as well determined from these studies. Since the concentrations of $Ru^{III}ORu^{III}$ and $Ru^{V}ORu^{V}$ were very low, their spectral contributions could be ignored while fitting the autocatalytic oxidation of $Ru^{III}ORu^{IV}$. However, the tailing contribution of Ce^{IV} was included as a known spectrum in the fitting procedure.

S0020-1669(97)00393-5 CCC: $14.00

Scheme 1

(a) $Ru^{III}ORu^{III} + Ce^{IV} \xrightarrow{k_1\ (2\times10^4)} Ru^{III}ORu^{IV} + Ce^{III}$

(b) $Ru^{III}ORu^{IV} + Ce^{IV} \xrightarrow{k_2\ (15)} Ru^{IV}ORu^{IV} + Ce^{III}$

(c) $Ru^{III}ORu^{IV} + Ru^{IV}ORu^{V} \underset{k_{-3}\ (\geq 10^5)}{\overset{k_3\ (7.3\times10^3)}{\rightleftharpoons}} 2\ Ru^{IV}ORu^{IV}$

(d) $Ru^{IV}ORu^{IV} + Ce^{IV} \xrightarrow{k_4\ (\geq 10^5)} Ru^{IV}ORu^{V} + Ce^{III}$

(e) $Ru^{IV}ORu^{V} + Ce^{IV} \xrightarrow{k_5\ (\geq 10^2)} Ru^{V}ORu^{V} + Ce^{III}$

(f) $Ru^{V}ORu^{V} + 2\ H_2O \xrightarrow{k_6\ (\geq 1\ s^{-1})} Ru^{III}ORu^{III} + O_2$

(g) $Ru^{III}ORu^{III} + Ru^{IV}ORu^{V} \xrightarrow{k_7\ (\geq 10^6)} Ru^{III}ORu^{IV} + Ru^{IV}ORu^{IV}$

(h) $2\ Ru^{IV}ORu^{V} \underset{k_{-8}\ (< 22)}{\overset{k_8\ (22)}{\rightleftharpoons}} Ru^{IV}ORu^{IV} + Ru^{V}ORu^{V}$

solid is unstable with regard to O_2 evolution and redissolution to give $Ru^{III}ORu^{IV}$. The suspension was reduced to $Ru^{III}ORu^{III}$ by titration with just 3 equiv of ferrous ion since some of the catalyst was lost due to water oxidation.

The available spectral, electrochemical, structural, and resonance Raman data provide evidence for oxidation states $Ru^{III}ORu^{III}$, $Ru^{III}ORu^{IV}$, $Ru^{IV}ORu^{V}$, and $Ru^{V}ORu^{V}$ with the latter in the dioxo form $[(bpy)_2(O)Ru^{V}ORu^{V}(O)(bpy)_2]^{4+}$. By including $Ru^{IV}ORu^{IV}$ as a kinetic intermediate, it is possible to explain the autocatalysis in Figure 1 via the reactions in Scheme 1 (all values shown are second-order rate constants in $M^{-1}\ s^{-1}$ at 25 °C unless otherwise noted). For clarity, these reactions are not balanced in protons. The balanced reaction for water oxidation in eq. f is, for example,

$$[(bpy)_2(O)Ru^{V}ORu^{V}(O)(bpy)_2]^{4+} + 2H_2O \rightarrow [(bpy)_2(H_2O)Ru^{III}ORu^{III}(H_2O)(bpy)_2]^{4+} + O_2$$

The rate constants k_2, k_3, and k_8 were refined from a global fit to the spectral-kinetic data (340−680 nm) for the reaction in Figure 1, while the remaining rate constants were held fixed at values determined from independent kinetic experiments or estimated from kinetic simulations to produce both autocatalysis with 2 equiv of Ce^{IV} and pseudo-zero-order kinetics for consumption of large excesses of Ce^{IV}. The rate constants k_1 and k_7 (lower limit) were obtained directly from stopped-flow kinetic measurements. The stoichiometric cross reaction (eq 2) was too fast to measure ($t_{1/2} < 1$ ms), the only products

$$2Ru^{III}ORu^{III} + Ru^{IV}ORu^{V} \rightarrow 3Ru^{III}ORu^{IV} \qquad (2)$$

being $Ru^{III}ORu^{IV}$ and some unreacted $Ru^{III}ORu^{III}$.[10] The rate constants k_5 and k_6 were obtained from an experiment involving the addition of 5 equiv of Ce^{IV} to a solution of 5×10^{-5} M $Ru^{IV}ORu^{V}$ at pH 0. This resulted in the formation of $Ru^{III}ORu^{IV}$ ($t_{1/2} \sim 5$ s) without evidence of intermediates, indicating that oxidation of $Ru^{IV}ORu^{V}$ is the rate-determining step in this part of the cycle. Since the oxygen evolution process is not rate determining, the kinetic studies do not reveal anything about its mechanism. For simplicity, the 4-electron reduction of $Ru^{V}ORu^{V}$ has been included in the model as a single step ($k_6 > 1\ s^{-1}$). Subsequently, $Ru^{III}ORu^{III}$ is rapidly reoxidized to $Ru^{III}ORu^{IV}$ either by Ce^{IV} or higher oxidation states of the dimer (*e.g.*, eq 2). The rate constant ratio $k_3/k_{-3} \sim 0.1$ was chosen to be consistent with electrochemical studies that indicate that $Ru^{IV}ORu^{IV}$ is unstable with respect to disproportionation.[2b] The value of $k_4 > k_3$ is required to produce the autocatalytic formation of $Ru^{IV}ORu^{V}$ while maintaining $Ru^{IV}ORu^{IV}$ at a relatively low concentration, as suggested by the nearly isosbestic behavior of the experimental data. The rate constant k_8 for disproportionation of $Ru^{IV}ORu^{V}$ is required to model the tailing portion of the reaction after consumption of Ce^{IV}. However, k_{-8} never contributes significantly owing to the low concentrations of $Ru^{IV}ORu^{IV}$ and $Ru^{V}ORu^{V}$. Since there is a high degree of coupling among the kinetic processes the derived rate constants cannot be determined uniquely. While individual fits produce standard errors of 1−3% for the adjustable rate constants, replicate runs gave ranges of 20% for k_3 and 100% for k_2 and k_8, respectively.

Some of the highlights in Scheme 1 are as follows: (1) $Ru^{V}ORu^{V}$ does not build up because its loss via water oxidation (eq f) is rapid compared to its formation (eq e). (2) $Ru^{III}ORu^{III}$ does not appear during catalysis because of rapid comproportionation with $Ru^{IV}ORu^{V}$ (and $Ru^{V}ORu^{V}$) to give $Ru^{III}ORu^{IV}$ (eq g). (3) There is autocatalysis because oxidation of $Ru^{IV}ORu^{IV}$ to $Ru^{IV}ORu^{V}$ by Ce^{IV} (eq d) is more rapid than oxidation of $Ru^{III}ORu^{IV}$ to $Ru^{IV}ORu^{IV}$ (eq b); after the reaction begins, $Ru^{IV}ORu^{IV}$ forms by comproportionation (eq c). (4) There is a distribution between $Ru^{III}ORu^{IV}$ and $Ru^{IV}ORu^{V}$ during catalysis with excess Ce^{IV}. Although counterintuitive, $Ru^{IV}ORu^{V}$ is favored with time as Ce^{IV} is depleted. This is because the rate-limiting step changes from oxidation of $Ru^{III}ORu^{IV}$ by comproportionation to oxidation of $Ru^{IV}ORu^{V}$ by Ce^{IV} as the reaction proceeds to completion.

It is interesting to compare the blue dimer with the oxygen-evolving complex (OEC) of photosynthesis. In the OEC, sequential absorption of four photons accompanied by electron transfer leads from the S_0 state to the S_4 state followed by water oxidation.[4] Four Mn ions are involved. In the blue dimer, sequential oxidation occurs from $Ru^{III}ORu^{III}$ to $Ru^{V}ORu^{V}$ with loss of four electrons and four protons followed by rapid O_2 evolution. Access to doubly oxidized Ru centers requires terminal oxo formation in the highest oxidation state.

Acknowledgment. We thank the National Institutes of Health for financial support of this work under Grant No. 5-R01-GM32296. We also thank Dr. Martin Devenney for assistance with the Raman experiments.

IC970393B

(10) The cross reaction was studied by sequential mixing, stopped-flow measurements where $Ru^{III}ORu^{III}$ was first oxidized with 2 equiv of Ce^{IV} at pH 0, followed by mixing with a third solution of $Ru^{III}ORu^{III}$ after a dwell time of 45 s.